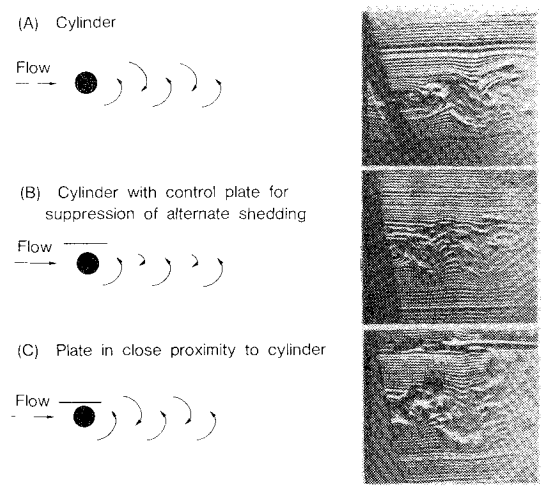

Fig. 2 Qualification of vortex suppression in freestream.

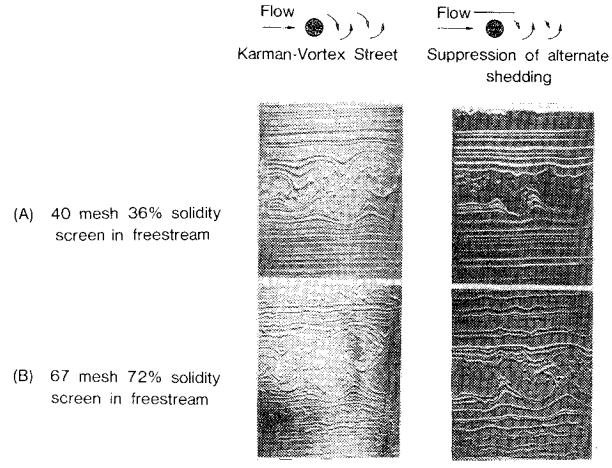

Fig. 3 Qualification of vortex suppression in a turbulent flowfield.

Figure 2 shows the results of the study in the freestream. The left side of the figure shows sketches of the proposed flow downstream of the device, and on the right side are the corresponding streakline patterns photographed in the tunnel. The cylinder alone produced the expected Karman-Vortex street. The cylinder/flat plate arrangement produced different patterns depending on the relative displacement between them. With the spacing of the optimum configuration there was evidence of suppression of alternate shedding of vorticity. When the components were too close, the streakline pattern corresponded to a single body. Not shown is the case where the components were too far apart—this simply produced separate patterns for each piece.

To answer the question of what happens to the suppression when the cylinder and adjacent plate are placed in a more turbulent flowfield (initial $U'_\infty/\bar{U} \simeq 0.03\%$), screens of varying mesh and percent solidity were placed 25.4 cm upstream of the cylinder. The entire process of photographing the vortex patterns downstream of various configurations was then repeated. Figure 3 shows typical results for two different screens: screen A was 40 mesh and had a solidity of 35%, screen B was 57 mesh and had a solidity of 72%. In all cases, the turbulence from the screens had little, if any, effect on the suppression mechanism of the cylinder/adjacent plate configuration.

Conclusions

The placement of a relatively short-chord, flow-aligned plate in the proximity of a cylinder allows the production of nearly "one-sided" or "one-signed" oscillatory transverse control vortices. The turbulence level of the incoming freestream has little effect on the suppression of the shed vorticity within the range considered in this study.

References

[1]Roshko, A., "Structure of Turbulent Shear Flows: A New Look," AIAA Paper 76-78, Jan. 1976.

[2]Bushnell, D.M., "Turbulent Drag Reduction for External Flows," AIAA Paper 83-0227, Jan. 1983.

[3]Bushnell, D.M., "Body-Turbulence Interaction," AIAA Paper 84-1527, June 1984.

[4]Sajben, M., Chen, C.P., and Kroutil, J.C., "A New, Passive Boundary Layer Control Device," AIAA Paper 76-700, July 1976.

[5]Covery, E.E. and Kanevsky, A.R., "Preliminary Experiment Designed to Support a Feasibility Demonstration of a Novel Method for Developing Unsteady Boundary Layer Profiles," AFOSR-78-0901TR, 1978.

[6]Taneda, S., "Experimental Investigation of Vortex Streets," *Journal of the Physical Society of Japan,* Vol. 20, 1965, pp. 1714-1721.

[7]Vitale, A., "Vortex Shedding of a Circular Cylinder in Ground Effect," Von Karman Institute for Fluid Dynamics, Tech. Note 124, Feb. 1978.

[8]Kiya, M. and Arie, M., "Note on Helmholtz Instability of Vortex Street," Kokkaido University, *Faculty of Engineering Memoirs,* Vol. 15, Jan. 1979, pp. 43-47.

[9]Selahittin, G., "The Drag and Lift Characteristics of a Cylinder Placed Near a Plane Surface,' M.S. Thesis, Naval Postgraduate School, Monterey, CA, Dec. 1975.

[10]Zdravkovich, M.M., "Observation of Vortex Shedding Behind a Towed Circular Cylinder Near a Wall," *Third International Symposium on Flow Visualization,* Ann Arbor, MI, Sept. 1983, pp. 391-395.

[11]Kambe, T., "A Class of Exact Solutions of Two-Dimensional Viscous Flow," *Journal of the Physical Society of Japan,* Vol. 52, March 1983, pp. 834-841.

[12]Kiya, M. and Arie, M., "Formation of Vortex Street in a Laminar Boundary Layer," *Journal of Applied Mechanics,* Vol. 47, June 1980, pp. 227-233.

[13]Freymuth, P., Bank, W., and Palmer, M., "First Experimental Evidence of Vortex Splitting," *The Physics of Fluids,* Vol. 27, May 1984, pp. 1045-1046.

[14]Morton, B.R., "The Generation and Decay of Vorticity," *Geophysical and Astrophysical Fluid Dynamics,* Vol. 28, 1984, pp. 277-308.

[15]Corke, T., Koga, D., Drubka, R., and Nagib, H., "A New Technique for Introducing Controlled Sheets of Smoke Streaklines in a Wind Tunnel," *International Congress of Instrumentation in Aerospace Simulation Facilities,* Shrivenham, England, Sept. 1977, Record (A79-15651-04-35), IEEE, New York, 1977, pp. 74-80.

Influence of Trailing-Edge Meshes on Skin Friction in Navier-Stokes Calculations

Werner Haase*
Dornier GmbH, Friedrichshafen
Federal Republic of Germany

Introduction

FROM recent investigations concerning numerical solutions of the Navier-Stokes equations for transonic turbulent flows over airfoils one can easily conclude that accurate

Received Aug. 7, 1985; revision received Dec. 26, 1985.

*Research Scientist.

prediction of skin-friction distributions is a difficult task. Moreover, especially in the trailing-edge region, contributions known to the author either concern with an upper-surface skin-friction distribution increasing dramatically at the trailing edge, or skin-friction results are not shown in the trailing-edge region. In some cases, where a drastic increase can be observed, it is often accompanied by local streamwise pressure oscillations. In Refs. 1-4, the skin friction increases near the airfoil trailing edge, although in all cases the flow should decelerate due to a positive pressure gradient along the upper surface. Whereas in Refs. 5-8 the skin-friction behavior near the trailing edge is not shown. In all of these contributions, which are assumed to be representative of that field of research, no special trailing-edge problems have been reported.

All referenced investigators[1-8,10,11,13] solve the time-averaged Navier-Stokes equations by means of finite difference or finite volume methods using O-, C- and H-type meshes for geometrical discretization. Therefore, it might be straightforward to argue that the trailing-edge problem is not related to a certain mesh type or a special numerical formulation. Furthermore, use of different types of turbulence models does not really affect the skin friction near the trailing edge as is shown in detail in Ref. 2.

Present Results

In the present Note, an attempt will be made to interpret the trailing-edge skin-friction distribution with respect to the mesh structure (definitely not to the mesh type) in the trailing-edge vicinity of the RAE 2822 airfoil. All calculations are performed at a Mach number of 0.73, Reynolds number of 6.5 million, and an angle of attack of 3.19 deg, representing the original properties of the RAE 2822 (test case 9).[9] Results for that test case (also used in the 1980 Stanford Conference) are presented in Refs. 2, 7, and 8.

In the present investigation, the computational method used to solve the Navier-Stokes equations for compressible flow in full conservation form is the finite volume method according to Ref. 10. Rewriting the Navier-Stokes equations in integral form and dividing the computational domain into quadrilateral cells one obtains a system of ordinary differential equations by applying the integral equations to each cell separately.[10] The set of ordinary differential equations in time is solved by means of an explicit four-stage Runge-Kutta time-stepping method. To control an odd-even decoupling, a Shuman-type filter is introduced with no special treatment at the trailing edge. Due to the fact that only the steady state is of interest, the difference equations are solved by a local time-stepping approach based on the maximum allowable time step for each cell (CFL number = 2.8). Introducing the residual averaging approach,[11] i.e., collecting the information from residuals implicitly, gives rise to a higher CFL number, which has been chosen to be 5.0 for all calculations. The viscous terms are treated using central differences throughout the domain and one-sided formulas are used at the surface.

The steady state is defined to have occurred when the force coefficients (drag and lift) do not vary more than 0.05% and the total number of supersonic points remains constant within a monitoring sequence of 15 iterations. Typically, an error norm reduction (L2-norm of d_ρ/dt) of 3 to 4 decades is reached and lift and drag coefficients as well as the number of supersonic points approach an asymptotic value. In order to model turbulent flow structures, an algebraic (zero-equation) turbulence model[12] is applied.

For discretization of the computational domain, a C-type mesh is used with 100 mesh points for surface representation. The mesh spacing normal to the surface is geometrically stretched. A constant number of 16 mesh points is distributed across the boundary layer to ensure proper resolution of the viscous layer; a total of 44 grid points are used in the normal direction of the grid. The y^+ value (in terms of the law of the wall for the first grid point adjacent to the surface) is less than 6. The far-field boundary is located at a distance of approximately 20 chord lengths. Variations to this mesh are performed only in the region behind the airfoil concerning especially the angle of the trailing-edge meshline. In Fig. 1, the trailing-edge region of one of those meshes is shown. The trailing-edge meshline emanates, with respect to the chordline, at 0 deg.

Based on the mesh plotted in Fig. 1, careful checks of the RAE 2822 (case 9) computations clearly demonstrate that the trailing-edge streamline emanates at 0 deg as well, thus coinciding with the trailing-edge meshline. As will be discussed in the following, aligning meshes with the trailing-edge streamline produces plausible flowfield predictions. Varying the slope of the trailing-edge meshline from −7.4 deg (bisector) via −3.0 deg (lower edge angle) to 0.0 deg (streamline case, see Fig. 1), and furthermore to 1.7 deg (for trial), results in different skin-friction distributions at the rear end of the RAE 2822 airfoil as shown in Fig. 2. It can clearly be seen that only marginal changes occur until approximately 95% of the chordlength is reached, causing a likewise unchanged pressure and velocity field in that area. At the last 5% of the airfoil, however, different types of skin-friction distributions are obtainable. It should be noted at this point that, due to the finite volume approach, the skin friction in Fig. 2 can be accurately plotted only up to the last surface volume. Skin friction is computed at the side center of all surface volumes and intentionally no extrapolation has been applied to determine an appropriate value for skin friction at 100% of chordlength. If

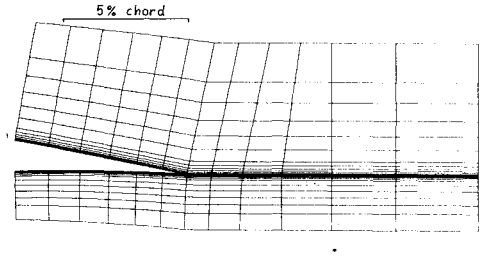

Fig. 1 Computational mesh in the trailing-edge vicinity of the RAE 2822 airfoil (case 9) using a trailing-edge meshline aligned with the trailing-edge streamline.

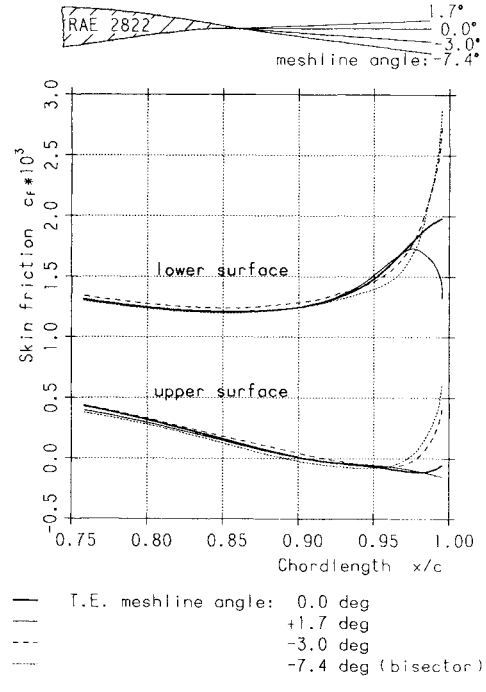

Fig. 2 Trailing-edge skin-friction distributions for the RAE 2822 airfoil (case 9) and various trailing-edge meshline angles.

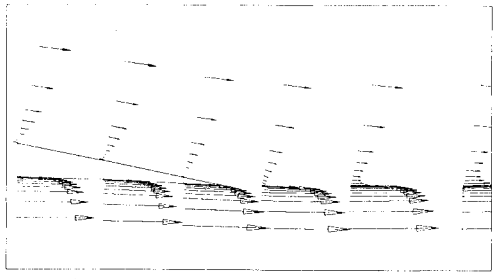

Fig. 3 Velocity vector plot for the RAE 2822 airfoil (case 9) in the trailing-edge vicinity.

severe changes in the skin-friction distribution can be observed, as demonstrated in Fig. 2 for negative meshline angles, streamwise oscillations in the pressure near the trailing edge increase both on the airfoil and in the near wake.[8,10] Some streamline oscillations have also been reported in Ref. 13 studying the near-wake behavior behind an airfoil, although wake alignment has been used.

Consequently, for the RAE 2822 (case 9), negative trailing-edge meshline angles result in an increase in skin friction along the upper and lower surfaces, while the situation is reversed for positive angles on both surfaces. Extrapolation of the plotted skin-friction distributions "by eye" shows that the separated flow (separation occurs at 90% of chordlength) "reattaches" at the trailing edge for a meshline emanation angle coinciding with the trailing-edge streamline. There is, in fact, no physical need for that, although examination of all given skin-friction distributions clearly show that physically plausible distributions on both the upper and lower surfaces appear only for the streamline angle case (0 deg). For all other meshline angles, the skin friction either increases on the upper surface or decreases on the lower surface; this is unexplainable from a physical point of view. Furthermore, use of negative meshline angles leads to an increase in streamwise pressure oscillations on the upper surface. For the streamline case and also for the 1.7-deg case, extremely small oscillations in pressure (an order of magnitude smaller, as reported in Ref. 13) can be observed. Although these differences influence the flow behavior in the trailing-edge region (on the surface as well as in the wake), their effect on force coefficients is negligible.

In addition, based on the computations for the streamline mesh angle, Fig. 3 presents the corresponding velocity vector plot, representing the flowfield within the boundary layer in the trailing-edge vicinity. It demonstrates the highly decelerated flow along the upper surface with the embedded small separated region as well as the accelerated flow along the lower surface and the mixing of both shear layers.

One might argue that the given results are directly related to the numerical procedure used in the present approach. Therefore, based on the bisector angle mesh, some other tests have been performed:

1) A special filtering technique has been used at the trailing edge, switching between central and one-sided filtering.

2) The filter has been switched off in cells adjacent to the surface in order to check the filter influence on the physical wall properties.

3) For the computation of the viscous terms, central and one-sided differences have been applied.

4) A refined mesh at the trailing edge as well as a new mesh with approximately 200 surface points and 25 grid points within the boundary layer have been used.

In all of the test cases mentioned no qualitative changes in the skin friction near the trailing edge are observable—only marginal quantitative changes occur. Especially for refined meshes in the trailing-edge region the influence on the skin-friction increase is of minor importance. Unfortunately, a comparison with measurements is not possible in the trailing-edge region because the last measuring point is at 90% of chord.

Conclusions

The present calculations delivered the most sensible results for skin friction as well as for pressure distributions in the case of aligning the trailing-edge mesh with the flow direction. The results are nearly independent of mesh type, finite approach, filtering technique, and turbulence model. Therefore, using wakeline-adapted meshes, some trailing-edge problems, e.g., the increase of skin friction as well as the increase in pressure oscillations, can be overcome and physically plausible flowfield predictions can be performed even in those highly viscous interaction regions.

Acknowledgment

This work was sponsored by the German Ministry of Defence (Rüfo 4) under Contract T/R41/D0007/D1407.

References

[1]Baldwin, B. S. and Lomax, H., "Thin Layer Approximation and Algebraic Model for Separated Turbulent Flows," AIAA Paper 78-257, Jan. 1978.

[2]Coakley, T. J., "Turbulence Modeling Methods for the Compressible Navier-Stokes Equations," AIAA Paper 83-1693, July 1983.

[3]Swanson, R.C. and Turkel, E., "A Multistage Time-Stepping Scheme for the Navier-Stokes Equations," AIAA Paper 85-0035, Jan. 1985.

[4]Schäfer, O., Frühauf, H-H., Bauer, B., and Guggolz, M., "Application of a Navier-Stokes Analysis to Flows Through Plane Cascades," ASME Paper 85/GT-56, 1985.

[5]Rubesin, M.W. et al., "An Experimental and Computational Investigation of the Mean and Dynamic Flow Field About an Airfoil in Supercritical Flow with Turbulent Boundary-Layer Separation," ICAS Paper 76-15, Oct. 1976.

[6]Deiwert, G.S., McDevitt, J.B., and Levy Jr., L.J., "Simulation of Turbulent Transonic Separated Flow Over an Airfoil," *Proceedings of the NASA Conference on Aerodynamic Analysis Requiring Advanced Computers,* Langley, VA, NASA SP-347, 1975.

[7]Mehta, U., "Reynolds Averaged Navier-Stokes Computations of Transonic Flows Around Airfoils," *Second Symposium on Numerical and Physical Aspects of Aerodynamic Flows,* Long Beach, CA, Jan. 1983.

[8]Haase, W., Misegades, K., and Naar, M., "Adaptive Grids in Numerical Fluid Dynamics," *International Journal for Numerical Methods in Fluids,* Vol. 5, No. 6, 1985, pp. 515-528.

[9]Cook, P.H., McDonald, M.A., and Firmin, M.C.P., "Aerofoil RAE 2822—Pressure Distributions and Boundary Layer and Wake Measurements," AGARD-AR-138, 1979, pp. A6-1 to A6-77.

[10]Haase, W., Wagner, B., and Jameson, A., "Development of a Navier-Stokes Method Based on a Finite Volume Technique for the Unsteady Euler Equations," *Notes on Numerical Fluid Mechanics,* Vol. 7, Vieweg-Verlag, 1983, pp. 99-107.

[11]Jameson, A., "The Evolution of Computational Methods in Aerodynamics," Princeton University, Princeton, NJ, MAE Rept. 1608, May 1983.

[12]Stock, H. W., "An Eddy Viscosity Model for Attached and Slightly Detached Flows in Navier-Stokes Computations," *Turbulence Modelling for Incompressible Flows,* EUROMECH 180, Karlsruhe, FRG, 1984.

[13]Deiwert, G. S., "Computation of Turbulent Near Wake for Asymmetric Airfoils," *Proceedings of the 4th US-FRG Meeting on Viscous and Interacting Flow Field Effects,* Forschungsberichte aus der Wehrtechnik, BMVg-FBWT 79-31, 1979, pp. 455-467.